Experimental Realization of Self-Contained Quantum Refrigeration

Keyi Huang,[1] Cheng Xi,[1,2] Xinyue Long,[1,3] Hongfeng Liu,[1] Yu-ang Fan,[1] Xiangyu Wang,[1] Yuxuan Zheng,[1] Yufang Feng,[1] Xinfang Nie,[1,3,*] and Dawei Lu[1,3,4,†]

[1]*Shenzhen Institute for Quantum Science and Engineering and Department of Physics, Southern University of Science and Technology, Shenzhen 518055, China*

[2]*Department of Physics, City University of Hong Kong, Tat Chee Avenue, Kowloon, Hong Kong SAR, China*

[3]*Quantum Science Center of Guangdong-Hong Kong-Macao Greater Bay Area, Shenzhen 518045, China*

[4]*International Quantum Academy, Shenzhen 518055, China*

(Received 19 December 2023; accepted 16 April 2024; published 23 May 2024)

A fundamental challenge in quantum thermodynamics is the exploration of inherent dimensional constraints in thermodynamic machines. In the context of two-level systems, the most compact refrigerator necessitates the involvement of three entities, operating under self-contained conditions that preclude the use of external work sources. Here, we build such a smallest refrigerator using a nuclear spin system, where three distinct two-level carbon-13 nuclei in the same molecule are involved to facilitate the refrigeration process. The self-contained feature enables it to operate without relying on net external work, and the unique mechanism sets this refrigerator apart from its classical counterparts. We evaluate its performance under varying conditions and systematically scrutinize the cooling constraints across a spectrum of scenarios, which sheds light on the interplay between quantum information and thermodynamics.

DOI: 10.1103/PhysRevLett.132.210403

Introduction.—Ever since Carnot's pioneering exploration of steam engines, which laid the foundation for thermodynamics, how to efficiently extract additional heat from an already cooled system has remained a central concern. The progress in cooling techniques has unlocked doors to extraordinary phenomena that emerge at very low temperatures [1–3], and has played a pivotal role in advancing the engineering of quantum systems [4–10]. The paradigm shift to the quantum level has offered new perspectives on quantum thermodynamics [11–15], which leads to the conceptualization and experimental scrutiny of various quantum models [16–29]. At present, building an enhanced quantum refrigerator, characterized by heightened efficiency while remaining in compliance with the laws of thermodynamics, remains a paramount aspiration [30–35].

Unlike classical refrigerators, quantum refrigeration demands a consideration of thermodynamic properties at the microscopic scale. A well-known example is the effective temperature of a single spin, which is defined by its polarization. This, in turn, introduces spin's "cooling" algorithms by enhancing its polarization through quantum operations [36–39]. The efficacy of this cooling method is intricately linked to the scale and correlation of the spin bath [40], rendering it a promising avenue for the development of robust quantum refrigeration systems. Drawing from a similar concept, a cooling model involving three qubits has been devised to explore the concept of the smallest conceivable refrigerator [41]. This model incorporates the idea of self-containment, accentuating the refrigerator's operation without a reliance on external work sources [42].

In experimental studies, algorithmic cooling and related quantum refrigeration concepts have been demonstrated using nuclear magnetic resonance (NMR) [43,44] and nitrogen-vacancy centers in diamond [45]. However, the realization of the self-contained refrigeration, operating without reliance on external resources, has remained elusive. In this work, we experimentally implement such a self-contained refrigerator model, comprising two cooling spins and one target spin. This configuration represents the smallest self-contained refrigerator achievable with two-level systems [41]. Facilitated by the participation of three distinct spin-1/2 ^{13}C nuclei in the same molecule, the entire cooling process requires no external input of work, owing to the meticulously designed gaps between energy levels. To understand the underlying mechanism of this refrigerator, we scrutinize the changes that occur within each spin during the cooling process and construct a refrigeration cycle. Furthermore, we conduct the working condition analysis and determine its achievable limiting temperature.

Model.—The concept of self-containment is introduced in exploring the minimal scale of thermal machines, employing three two-level quantum systems [41]. Let us start from the cooling process without the self-contained condition, which involves two spins q_1 and q_2 at the same temperature T_0. They have zero ground-state energies, and excited-state energies at E_1 and E_2, where $E_1 < E_2$. The population of the ith spin ($i = 1, 2$) in the excited state is $e^{-\beta E_i}/\mathcal{Z}_i$, where $\beta = 1/k_B T_0$ is the inverse temperature, k_B is the Boltzmann constant, and $\mathcal{Z}_i = 1 + e^{-\beta E_i}$ is the partition function. At T_0, q_1 has a higher probability of

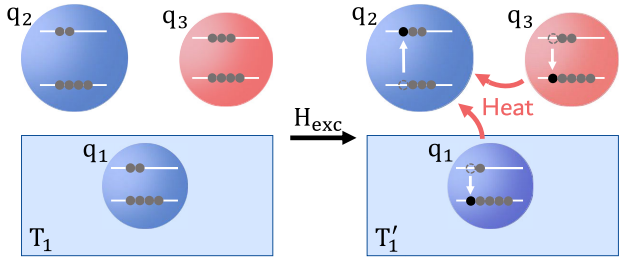

FIG. 1. Schematic representation of self-contained refrigeration designed to cool down the first spin, q_1. The energy distribution among the three spins satisfies $E_2 = E_1 + E_3$. The evolution under the Hamiltonian H_{exc} exchanges the population by $|010\rangle \leftrightarrow |101\rangle$. As a result, q_2 extracts heat from the other two spins, leading to the cooling of the target spin q_1 ($T_1' < T_1$).

being in the excited state compared to q_2 due to its smaller energy difference. If we apply a SWAP gate to exchange the states of q_1 and q_2, the temperature of q_1 becomes $T_0 E_1/E_2$. Since $E_1 < E_2$, the final temperature of q_1 is lower than its temperature T_0. As a result, q_1 undergoes cooling due to this population exchange.

In this particular scenario, the SWAP gate exchanges the two states, $|01\rangle \leftrightarrow |10\rangle$. It is evident that the SWAP gate necessitates an input of work due to the disparity in energy levels between these two states. Consequently, this cooling process for the two spins cannot be considered self-contained. To achieve self-contained cooling, the energy levels being exchanged must be degenerate, ensuring that the operation consumes no work. This requirement, in turn, necessitates the introduction of a third spin, q_3, with an excited-state energy at E_3.

When the energy relationship satisfies $E_2 = E_1 + E_3$, the joint states $|010\rangle$ and $|101\rangle$ become degenerate, meaning that the exchange of the two states requires no work input. Like the two-spin case, q_1 can be cooled down by this exchange, as depicted in Fig. 1. It can be realized through the evolution under the interaction Hamiltonian $\mathcal{H}_{\mathrm{exc}} = g(|010\rangle\langle 101| + |101\rangle\langle 010|)$, where g represents the interaction strength [41]. It is essential to note that such a Hamiltonian encompasses three-body interactions, which is not a natural term in real-world systems. Hence, it is imperative to employ control techniques that enable the realization of $\mathcal{H}_{\mathrm{exc}}$ in a physical system while maintaining the self-containment, which will be discussed later in this Letter.

Experimental setup.—Now, we delve into the physical system designed to realize self-contained refrigeration. We employ a nuclear spin system, where three distinct two-level ^{13}C nuclei are arranged in a chainlike molecular structure (crotonic acid dissolved in d_6 acetone) [46–48], to play the roles of the three spins in the refrigeration model. The experiment is conducted at room temperature using a Bruker 300 MHz NMR spectrometer. The internal Hamiltonian of the system can be written as $\mathcal{H}_{\mathrm{NMR}} = -\sum_i \omega_i \sigma_z^i/2 + \pi \sum_{i<j} J_{ij}\sigma_z^i\sigma_z^j/2$, where σ_z^i represents the Pauli matrix of the ith spin, ω_i is the Larmor frequency, and J_{ij} denotes the coupling strength between the ith and jth spins. Specific values for ω_i and J_{ij} can be found in Supplemental Material [48]. Additionally, we can apply transverse radio-frequency pulses to execute single-qubit rotations.

Starting from the thermal equilibrium state dictated by the NMR system Hamiltonian $\mathcal{H}_{\mathrm{NMR}}$, the first step involves creating the initial state ρ_0 for the refrigeration model [48]. In our experimental setup, we set the temperatures of three spins as $T_1 = T_2 = T_3/5$, where $T_1 = 2\delta/k_B$. The energy levels are defined as $E_1 = \delta$, $E_2 = 3\delta$, and $E_3 = 2\delta$ to satisfy the self-contained condition $E_2 = E_1 + E_3$. Here, δ serves as an arbitrary energy unit, and we set $\delta = 2$. Preparing ρ_0 under these specified parameters involves redistributing populations of ρ_{eq} through the application of non-unitary gates. We utilize single-qubit rotations to redistribute the corresponding populations and apply 1 ms z-gradient pulses to eliminate unwanted coherence, as illustrated in Fig. 2(a); see Supplemental Material for details [48].

Verification of self-containment.—The subsequent stage involves the evolution of the Hamiltonian $\mathcal{H}_{\mathrm{exc}} = g(|010\rangle\langle 101| + |101\rangle\langle 010|)$. To facilitate its implementation in the experiment, we rewrite it as

$$\mathcal{H}_{\mathrm{exc}} = \frac{g}{4}(\sigma_x^1\sigma_x^2\sigma_x^3 + \sigma_x^1\sigma_y^2\sigma_y^3 + \sigma_y^1\sigma_x^2\sigma_y^3 + \sigma_y^1\sigma_y^2\sigma_x^3). \quad (1)$$

Remarkably, all terms in Eq. (1) commute with each other, simplifying the simulation of this Hamiltonian and ensuring that the decomposition result is identical to that of the original Hamiltonian. Each three-body term can be further exactly decomposed into single- and two-qubit gates [49], as illustrated in Fig. 2(a), and a comprehensive pulse sequence is provided in Supplemental Material [48].

As $|010\rangle$ and $|101\rangle$ are degenerate, achieving their exchange during the evolution of $\mathcal{H}_{\mathrm{exc}}$ does not require any input work. However, in our experimental setup, we employ the quantum simulation approach to realize this evolution, necessitating radio-frequency pulses and corresponding energy transfer. To compute the energy transfer and verify the self-contained condition, we measure work and heat separately in each experimental step. Here, work involves the energy transfer from the three-spin system to some external repository without changing entropy, while heat entails energy exchanges that involve entropy changes [50]. Specifically, work and heat can be expressed as $dW = \mathrm{tr}(\rho dH)$ and $dQ = \mathrm{tr}(Hd\rho)$, respectively [51].

Without loss of generality, we show the measurement of work and heat during the application of one pulse. As depicted in Fig. 2(b), the thermodynamic change can be summarized into three steps. Assuming that the state is ρ_1 before applying the pulse, and the current Hamiltonian is

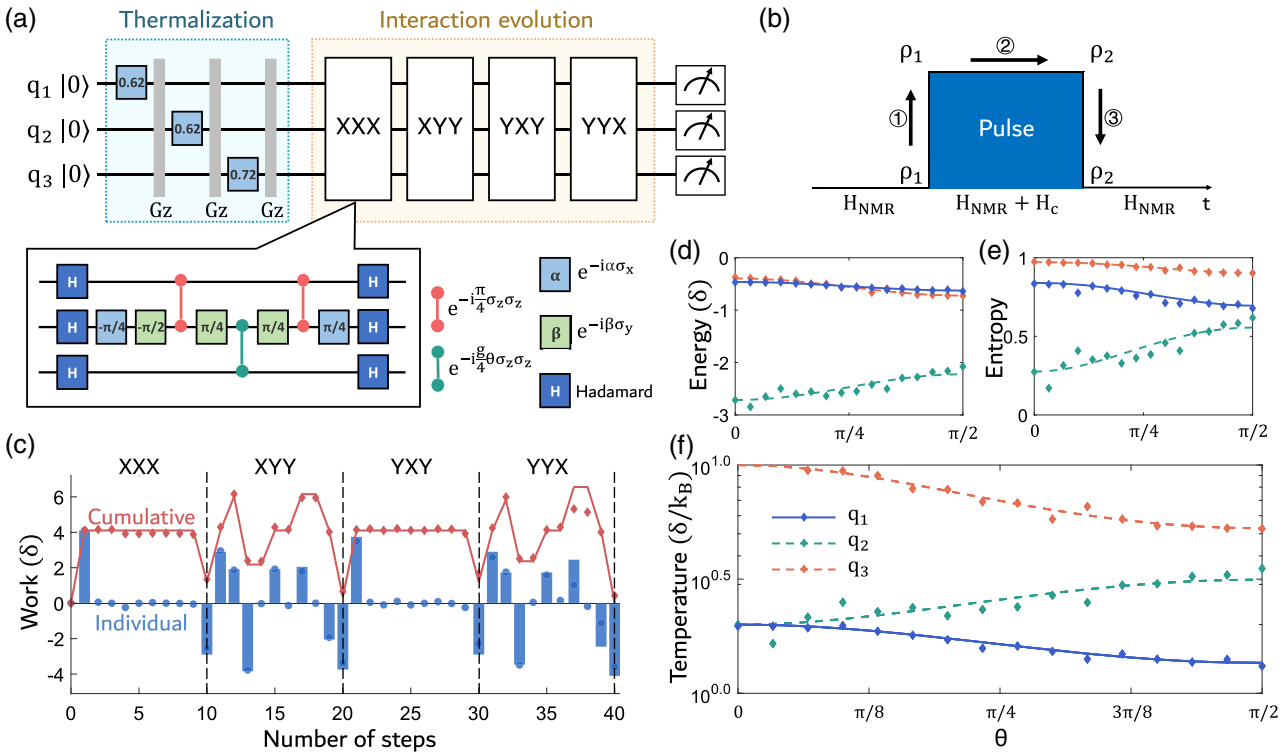

FIG. 2. (a) Quantum circuit for self-contained refrigeration. After preparing the initial thermal state ρ_0, the implementation of the $\mathcal{H}_{\text{exc}}$ evolution involves four three-body terms. Each term can be decomposed into ten steps comprising single- and two-qubit gates, as illustrated in the lower-left box. (b) Measurement of work and heat during the application of one pulse. The three steps correspond to dW_1, dQ_1, and dW_2, as defined in the main text. (c) Measured cumulative and individual work for the forty steps during the $\mathcal{H}_{\text{exc}}$ evolution. The total work sums up to zero when considering all individual work contributions, indicating that the refrigeration is self-contained. (d)–(f) Energy, entropy, and temperature of each spin during the $\mathcal{H}_{\text{exc}}$ evolution. The markers represent the experimental results. Entropy and energy transfer occur from q_1 and q_3 to q_2 over time, resulting in an increase in q_2's temperature and a decrease in the temperatures of the others.

$\mathcal{H}_{\text{NMR}}$. The first step is to apply the pulse, which introduces an additional Hamiltonian term $\mathcal{H}_c$. As the state remains unchanged, only work, expressed as $dW_1 = \text{tr}(\rho_1\mathcal{H}_c)$, is involved, and there is no heat transfer. Subsequently, in the second step, the state evolves under a new Hamiltonian, entailing only heat transfer $dQ_1 = \text{tr}[(\rho_2 - \rho_1)(\mathcal{H}_{\text{NMR}} + H_c)]$. Here, ρ_2 is the state after applying the pulse to ρ_1. In the third step, the pulse $\mathcal{H}_c$ vanishes, and the only work involved is given by $dW_2 = -\text{tr}(\rho_2\mathcal{H}_c)$. Consequently, the application of a pulse can be viewed as a combination of the above work and heat transfer. Moreover, it can be calculated that $dQ_1 = 0$ in the ideal case, so the net work equals to the change of internal energy of the three-spin system [48].

In the experiment, we measure the change in internal energy to determine the work for each of the forty steps during the implementation of the $\mathcal{H}_{\text{exc}}$ evolution. These cumulative and individual changes in work during the implementation are illustrated in Fig. 2(c). Notably, although some steps involve the consumption and storage of work, the total work amounts to zero upon accounting for all individual contributions. The result shows that the entire refrigeration process requires no input work, indicating its self-contained nature as we discussed in [48].

Performance.—Given the established setup, we have demonstrated that refrigeration occurs in a self-contained manner, which ultimately results in the cooling of the target spin q_1. However, the precise mechanisms governing this cooling process, as well as its performance under diverse conditions, remain unclear. Therefore, subsequent to preparing the thermal state for the entire system, we introduce a variable evolution time denoted as θ in $e^{-i\mathcal{H}_{\text{exc}}\theta}$ and monitor the state of each spin at various time points. In experiment, we measure the energy, entropy, and temperature of each spin at different θ, and the obtained results are depicted in Figs. 2(d)–2(f).

As time progresses, the disorder of q_1 diminishes as entropy decreases, akin to the "data compression" step in algorithmic cooling [38]. Simultaneously, the energy of q_1 is transferred to the other spins, resulting in a reduction in its temperature. When considering all three spins collectively, despite the absence of work in this cooling process, it complies with the second law of thermodynamics. Energy transfer takes place, accompanied by a heat flow from the higher-temperature spin (q_3) to the lower-temperature spin (q_2), which has the potential to drive an "engine." The refrigeration of q_1 is thus propelled by this engine

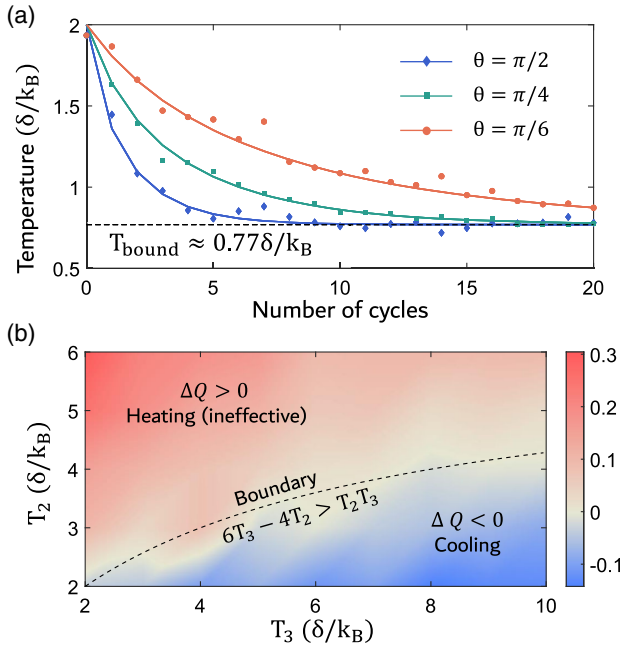

FIG. 3. (a) Temperature of the target spin q_1 for different numbers of refrigeration cycles at various evolution times θ. As θ increases (up to $\pi/2$, indicating a complete population exchange), the cooling time becomes shorter. Eventually, all cases converge to the same temperature, approximately $T_{\text{bound}} \approx 0.77\delta/k_B$, regardless of the evolution time. (b) Experimental heat transfer as a function of the temperatures of q_2 and q_3. The blue region represents heat released from q_1, leading to its cooling, and the red region represents heat absorbed by q_1. The dashed line indicates the predicted boundary between the two cases.

[21,48]. Consequently, spins q_1 and q_3 experience a decrease in temperature, while q_2 undergoes an increase. This thermodynamic perspective provides a clear picture of the refrigeration mechanism.

The refrigeration process can be extended into a cycle to achieve continuous cooling and attain and sustain the lowest temperatures. This cycle involves resetting q_2 and q_3 by bringing them into contact with their respective thermal environments and evolving the entire system under $\mathcal{H}_{\text{exc}}$ for the subsequent loop to further cool down the target spin q_1. When resetting these spins through contact, the heat in q_2, transferred from q_1 during refrigeration, will be dissipated into the environment. q_3 will absorb heat from the environment to restore its original states, akin to the discussion in Supplemental Material [48]. Figure 3(a) illustrates the temperature as a function of the cycle number n for various values of the evolution time θ. As n increases, the temperature of q_1 gradually decreases, indicating the effectiveness of the refrigeration cycle in continuously cooling down the target spin. Notably, with the evolution time θ increasing, the cooling efficiency improves, with q_1 experiencing the quickest cooling when $\theta = \pi/2$. This observation is expected, considering that $\theta = \pi/2$ implies a more complete information exchange.

Of particular interest is the fact that, irrespective of the evolution time θ within one cycle, all temperatures tend to converge to the same bounded value $T_{\text{bound}} \approx 0.77\delta/k_B$ after a finite number of cycles, as indicated by the dashed line in Fig. 3(a). This convergence underscores the limitation of this refrigeration process under these specific conditions, and we will delve into its underlying mechanism in the subsequent discussion.

Working conditions.—The decrease in the temperature of q_1 results from the evolution under the Hamiltonian $\mathcal{H}_{\text{exc}}$, which exchanges the population of states: $|010\rangle \leftrightarrow |101\rangle$. To ensure a lower temperature, the polarization of q_1 needs to be enhanced, implying that the population of q_1's excited state needs to decrease after this exchange. As only these two states are affected by this evolution, it is appropriate to exclusively consider them when analyzing the population change. For the initial thermal state, the populations of $|010\rangle$ and $|101\rangle$ are $P_{010} = e^{-\beta_2 E_2}/\mathcal{Z}_{\text{total}}$ and $P_{101} = e^{-\beta_1 E_1 - \beta_3 E_3}/\mathcal{Z}_{\text{total}}$, respectively. Here, $\mathcal{Z}_{\text{total}} = \mathcal{Z}_1\mathcal{Z}_2\mathcal{Z}_3$ represents the total partition function. Obviously, P_{010} corresponds to the probability for the ground state of q_1, while P_{101} is for the excited state. To increase q_1's polarization, $P_{101} > P_{010}$ is both a sufficient and necessary condition.

Consequently, the effective working condition for this refrigeration is given by

$$\frac{E_1}{T_1} + \frac{E_3}{T_3} < \frac{E_2}{T_2}. \tag{2}$$

This condition bears a resemblance to the second law of thermodynamics for quantum refrigerators [52]. Indeed, these concepts are interconnected through the specialized efficiency of this refrigerator [21].

In the cooling cycle, spins q_2 and q_3 are reset after each cycle, and their temperatures remain initially equal at the cycle's outset. Therefore, these temperatures can be considered constant throughout the entire refrigeration process. The cooling limitations of this cycle can be determined using Eq. (2) by fixing these two temperatures. We calculate that $T_1 > T_{\text{bound}}$ is the condition for successful refrigeration. If the temperature of q_1 satisfies this requirement, it will be cooled down in the subsequent cycle. Otherwise, the refrigeration process fails. Thus, this limitation represents the lowest temperature that can be reached using this cooling cycle, consistent with the experimental results depicted in Fig. 3(a). Importantly, this limitation is independent of the evolution time θ in each cycle, as the exchange is effective even in infinitesimally small time intervals. Once initiated, the temperature will continually decrease over subsequent cycles, eventually converging to this limitation.

This working condition is intricately linked to the temperatures of all three spins. The temperature of the target spin q_1 is particularly crucial as it establishes the cooling limitation over multiple cycles. Additionally, to comprehend how to maintain a system's low temperature, analyzing the refrigeration performance while

keeping q_1's temperature fixed becomes pivotal. To identify the proper conditions necessary for cooling the system at $2\delta/k_B$, we conduct experiments at varying temperatures T_2 and T_3. Maintaining the same energy differences as in the previous experiment and fixing q_1's temperature at $T_1 = 2\delta/k_B$, we execute a refrigeration process with $T_3 = [2\delta/k_B, 10\delta/k_B]$ and $T_2 = [2\delta/k_B, 6\delta/k_B]$. The heat transfer from q_1 is depicted in Fig. 3(b). The cooling process operates effectively when heat is released from this spin. This outcome aligns with Eq. (2). Consequently, we determine that the requirement for effective cooling is $6T_3 - 4T_2 - T_2T_3 > 0$ (with temperature units set to $\delta/k_B = 1$). Hence, we can establish the boundary where no heat transfer occurs at q_1 [dashed line in Fig. 3(b)]. The experimental results match well with the theoretical prediction, with the blue region signifying that refrigeration is valid under this setting and the red region indicating refrigeration failure.

Conclusion.—We demonstrate self-contained refrigeration using three nuclear spins through the NMR technique. In terms of dimensionality, this refrigerator is the smallest built using two-level systems [41]. By measuring the energy transfer during the evolution of the three-body interaction, we show that no net external work is needed to drive the refrigeration process, implying its self-containment. Additionally, we analyze the performance and mechanism of this refrigeration approach by monitoring the changes in energy, entropy, and temperature throughout the evolution, and additionally obtain the working condition of this refrigeration. Moreover, we delve into the potential implementation of this refrigeration cycle in quantum computation and its applicability within two solid-state spin systems [48]. The insights gained from our analysis can not only be extended to other thermodynamic models but also prove beneficial for other physical scenarios requiring the analysis of energy transfer, such as algorithmic cooling [53].

This work is supported by the National Key Research and Development Program of China (No. 2019YFA0308100); National Natural Science Foundation of China (No. 12104213, No. 12075110, No. 12204230); Science, Technology and Innovation Commission of Shenzhen Municipality (No. JCYJ20200109140803865, No. KQTD20190929173815000); Guangdong Innovative and Entrepreneurial Research Team Program (No. 2019ZT08C044); and Guangdong Provincial Key Laboratory (No. 2019B121203002);The Pearl River Talent Recruitment Program (No. 2019QN01X298); and Guangdong Provincial Quantum Science Strategic Initiative (No. GDZX2303001 and No. GDZX2200001).

*niexf@sustech.edu.cn
†ludw@sustech.edu.cn

[1] R. Combescot, *Superconductivity: An Introduction* (Cambridge University Press, Cambridge, England, 2022).
[2] K. B. Davis, M. O. Mewes, M. R. Andrews, N. J. van Druten, D. S. Durfee, D. M. Kurn, and W. Ketterle, Phys. Rev. Lett. **75**, 3969 (1995).
[3] M. H. Anderson, J. R. Ensher, M. R. Matthews, C. E. Wieman, and E. A. Cornell, Science **269**, 198 (1995).
[4] S. O. Valenzuela, W. D. Oliver, D. M. Berns, K. K. Berggren, L. S. Levitov, and T. P. Orlando, Science **314**, 1589 (2006).
[5] K. Y. Tan, M. Partanen, R. E. Lake, J. Govenius, S. Masuda, and M. Möttönen, Nat. Commun. **8**, 15189 (2017).
[6] Y. Nakamura, Y. A. Pashkin, and J. S. Tsai, Nature (London) **398**, 786 (1999).
[7] J. M. Martinis, S. Nam, J. Aumentado, and C. Urbina, Phys. Rev. Lett. **89**, 117901 (2002).
[8] M. Bal, C. Deng, J.-L. Orgiazzi, F. R. Ong, and A. Lupascu, Nat. Commun. **3**, 1324 (2012).
[9] C. L. Degen, F. Reinhard, and P. Cappellaro, Rev. Mod. Phys. **89**, 035002 (2017).
[10] B. Cheng, X.-H. Deng, X. Gu, Y. He, G. Hu, P. Huang, J. Li, B.-C. Lin, D. Lu, Y. Lu *et al.*, Front. Phys. **18**, 21308 (2023).
[11] E. Chitambar and G. Gour, Rev. Mod. Phys. **91**, 025001 (2019).
[12] J. M. R. Parrondo, J. M. Horowitz, and T. Sagawa, Nat. Phys. **11**, 131 (2015).
[13] J. Goold, M. Huber, A. Riera, L. del Rio, and P. Skrzypczyk, J. Phys. A **49**, 143001 (2016).
[14] S. Popescu, Nat. Phys. **10**, 264 (2014).
[15] X. Liu, D. Ebler, and O. Dahlsten, Phys. Rev. Lett. **129**, 230604 (2022).
[16] P. Skrzypczyk, N. Brunner, N. Linden, and S. Popescu, J. Phys. A **44**, 492002 (2011).
[17] J. P. Palao, R. Kosloff, and J. M. Gordon, Phys. Rev. E **64**, 056130 (2001).
[18] D. Felce and V. Vedral, Phys. Rev. Lett. **125**, 070603 (2020).
[19] X. Nie, X. Zhu, K. Huang, K. Tang, X. Long, Z. Lin, Y. Tian, C. Qiu, C. Xi, X. Yang, J. Li, Y. Dong, T. Xin, and D. Lu, Phys. Rev. Lett. **129**, 100603 (2022).
[20] L. Buffoni, A. Solfanelli, P. Verrucchi, A. Cuccoli, and M. Campisi, Phys. Rev. Lett. **122**, 070603 (2019).
[21] L. A. Correa, J. P. Palao, D. Alonso, and G. Adesso, Sci. Rep. **4**, 3949 (2014).
[22] P. G. Steeneken, K. Le Phan, M. J. Goossens, G. E. J. Koops, G. J. A. M. Brom, C. van der Avoort, and J. T. M. van Beek, Nat. Phys. **7**, 354 (2011).
[23] A. Mari and J. Eisert, Phys. Rev. Lett. **108**, 120602 (2012).
[24] G. Maslennikov, S. Ding, R. Hablützel, J. Gan, A. Roulet, S. Nimmrichter, J. Dai, V. Scarani, and D. Matsukevich, Nat. Commun. **10**, 202 (2019).
[25] J. P. S. Peterson, T. B. Batalhão, M. Herrera, A. M. Souza, R. S. Sarthour, I. S. Oliveira, and R. M. Serra, Phys. Rev. Lett. **123**, 240601 (2019).
[26] P. A. Camati, J. F. G. Santos, and R. M. Serra, Phys. Rev. A **99**, 062103 (2019).
[27] P. Skrzypczyk, A. J. Short, and S. Popescu, Nat. Commun. **5**, 4185 (2014).
[28] W. Ji, Z. Chai, M. Wang, Y. Guo, X. Rong, F. Shi, C. Ren, Y. Wang, and J. Du, Phys. Rev. Lett. **128**, 090602 (2022).
[29] K. Micadei, J. P. S. Peterson, A. M. Souza, R. S. Sarthour, I. S. Oliveira, G. T. Landi, T. B. Batalhão, R. M. Serra, and E. Lutz, Nat. Commun. **10**, 2456 (2019).

[30] N. Brunner, M. Huber, N. Linden, S. Popescu, R. Silva, and P. Skrzypczyk, Phys. Rev. E **89**, 032115 (2014).
[31] F. L. Curzon and B. Ahlborn, Am. J. Phys. **43**, 22 (1975).
[32] A. E. Allahverdyan, K. Hovhannisyan, and G. Mahler, Phys. Rev. E **81**, 051129 (2010).
[33] M. O. Scully, M. S. Zubairy, G. S. Agarwal, and H. Walther, Science **299**, 862 (2003).
[34] E. Geva and R. Kosloff, J. Chem. Phys. **96**, 3054 (1992).
[35] L. A. Correa, J. P. Palao, D. Alonso, and G. Adesso, Sci. Rep. **4** (2013).
[36] L. J. Schulman and U. V. Vazirani, in *Proceedings of the Thirty-First Annual ACM Symposium on Theory of Computing* (1999), pp. 322–329, 10.1145/301250.301332.
[37] J. M. Fernandez, S. Lloyd, T. Mor, and V. Roychowdhury, Int. J. Quantum. Inform. **02**, 461 (2004).
[38] P. O. Boykin, T. Mor, V. Roychowdhury, F. Vatan, and R. Vrijen, Proc. Natl. Acad. Sci. U.S.A. **99**, 3388 (2002).
[39] N. A. Rodríguez-Briones, J. Li, X. Peng, T. Mor, Y. Weinstein, and R. Laflamme, New J. Phys. **19**, 113047 (2017).
[40] N. A. Rodríguez-Briones, E. Martín-Martínez, A. Kempf, and R. Laflamme, Phys. Rev. Lett. **119**, 050502 (2017).
[41] N. Linden, S. Popescu, and P. Skrzypczyk, Phys. Rev. Lett. **105**, 130401 (2010).
[42] D. Venturelli, R. Fazio, and V. Giovannetti, Phys. Rev. Lett. **110**, 256801 (2013).
[43] J. Baugh, O. Moussa, C. A. Ryan, A. Nayak, and R. Laflamme, Nature (London) **438**, 470 (2005).
[44] C. A. Ryan, O. Moussa, J. Baugh, and R. Laflamme, Phys. Rev. Lett. **100**, 140501 (2008).
[45] R. R. Soldati, D. B. R. Dasari, J. Wrachtrup, and E. Lutz, Phys. Rev. Lett. **129**, 030601 (2022).
[46] X. Long, W.-T. He, N.-N. Zhang, K. Tang, Z. Lin, H. Liu, X. Nie, G. Feng, J. Li, T. Xin, Q. Ai, and D. Lu, Phys. Rev. Lett. **129**, 070502 (2022).
[47] T. Xin, L. Che, C. Xi, A. Singh, X. Nie, J. Li, Y. Dong, and D. Lu, Phys. Rev. Lett. **126**, 110502 (2021).
[48] See Supplemental Material at http://link.aps.org/supplemental/10.1103/PhysRevLett.132.210403 for further details on theoretical analysis and experimental procedures regarding self-contained refrigeration.
[49] C. H. Tseng, S. Somaroo, Y. Sharf, E. Knill, R. Laflamme, T. F. Havel, and D. G. Cory, Phys. Rev. A **61**, 012302 (1999).
[50] R. Uzdin, A. Levy, and R. Kosloff, Phys. Rev. X **5**, 031044 (2015).
[51] H. B. Callen, *Thermodynamics and an Introduction to Thermostatistics* (John Wiley & Sons, New York, 1991).
[52] A. Levy and R. Kosloff, Phys. Rev. Lett. **108**, 070604 (2012).
[53] N. A. Rodríguez-Briones and R. Laflamme, Phys. Rev. Lett. **116**, 170501 (2016).